Paper 12 Not open access : Characteristics of sulfated and carboxylated cellulose nanocrystal extracted from Juncus plant stems

Silahkan klik google drive utk full access:
https://drive.google.com/file/d/10s6vq4V0xjtuWpKxsCq9pUfJpopd8fZS/view?usp=sharing

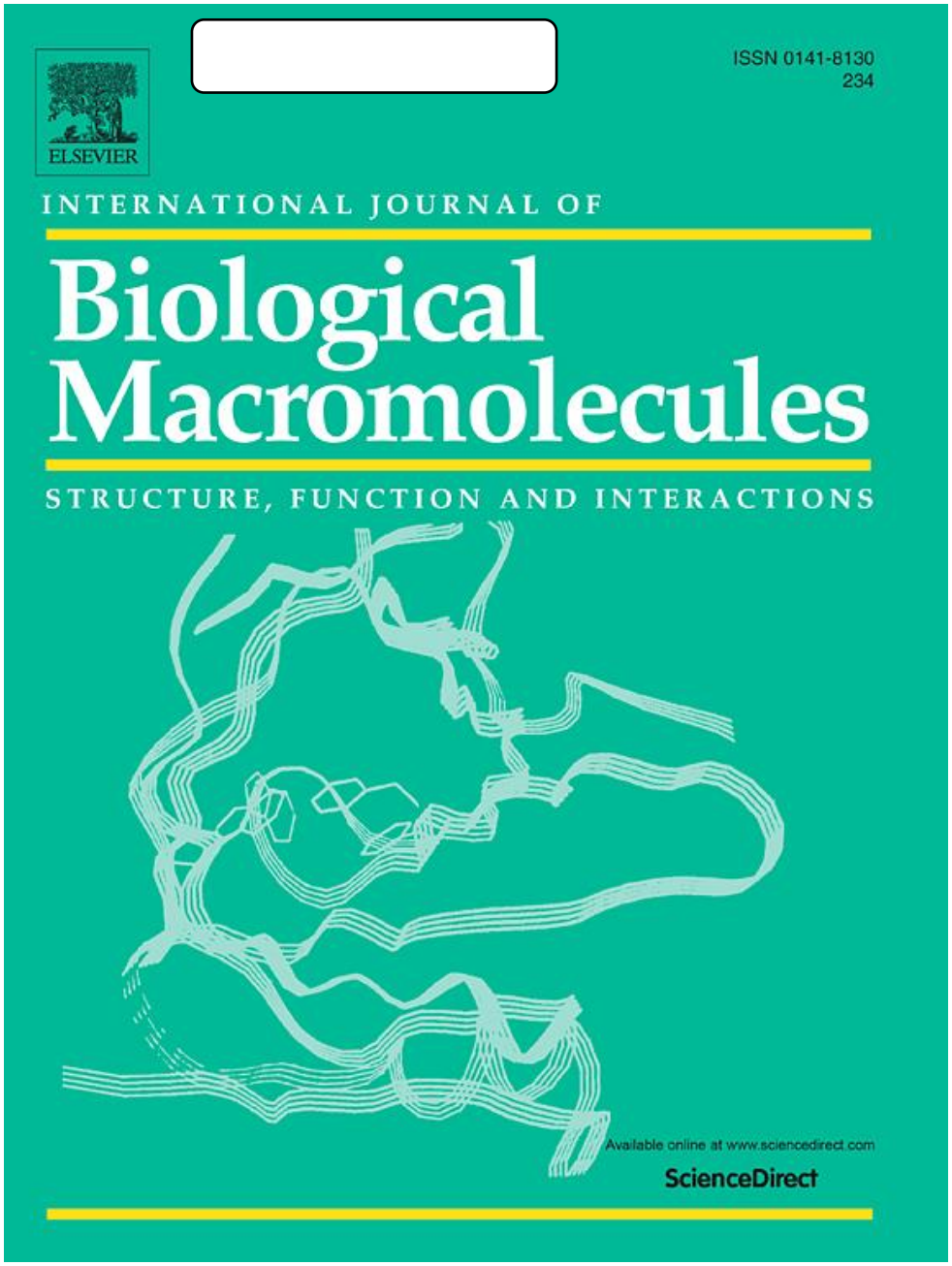

International Journal of Biological Macromolecules
Volume 154, 1 July 2020, Pages 1419-1425

Characteristics of sulfated and carboxylated cellulose nanocrystals extracted from *Juncus* plant stems

Zineb Kassab [a b], Edi Syafri [c], Youssef Tamraoui [a], Hassan Hannache [a b], Abou El Kacem Qaiss [d], Mounir El Achaby [a]

https://www.sciencedirect.com/science/article/abs/pii/S0141813019360702

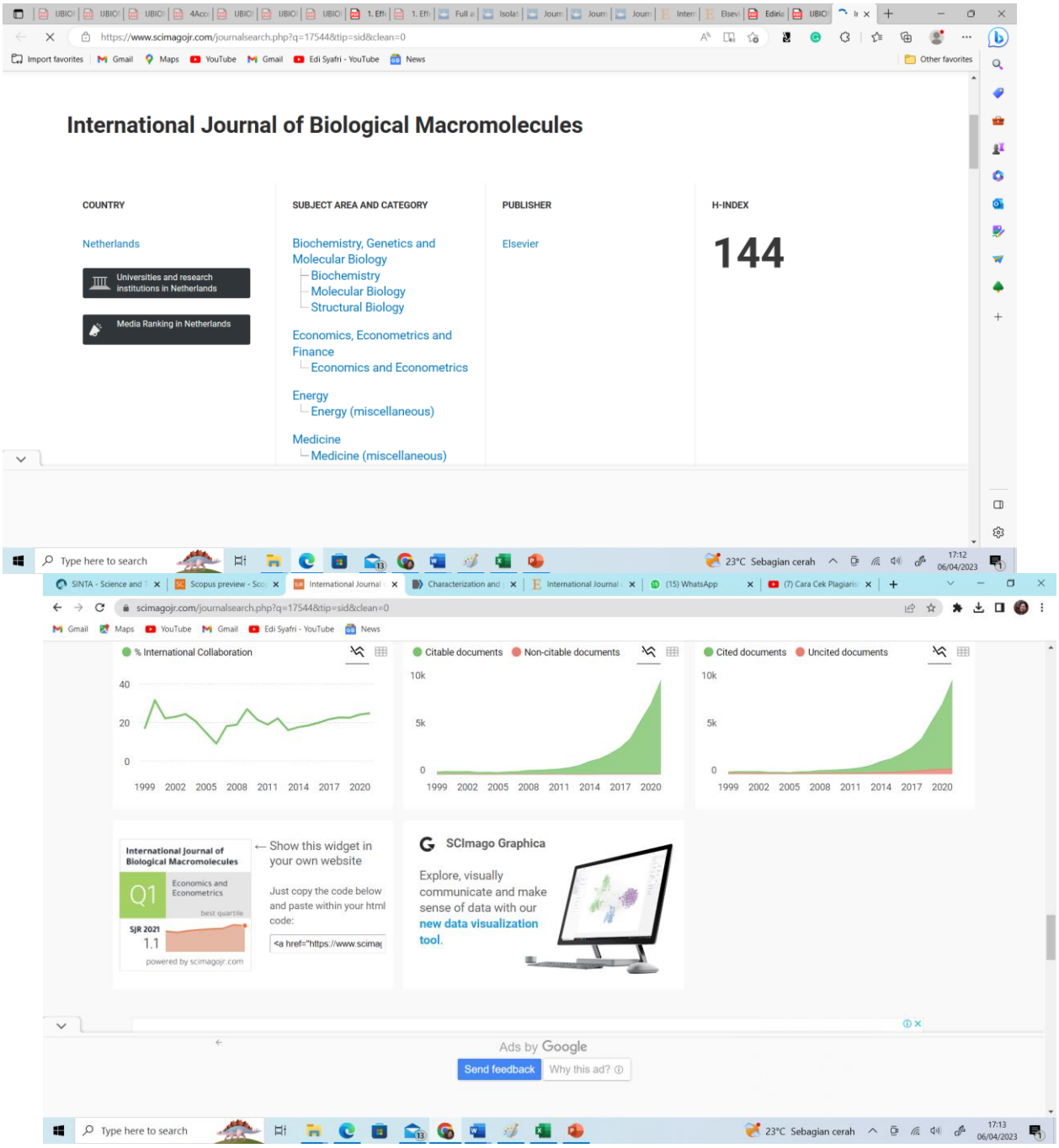
https://www.scimagojr.com/journalsearch.php?q=17544&tip=sid&clean=0
International Journal of Biological Macromolecules
COUNTRY
Netherlands
Universities and research institutions in Netherlands
Media Ranking in Netherlands
SUBJECT AREA AND CATEGORY
Biochemistry, Genetics and Molecular Biology
Biochemistry
Molecular Biology
Structural Biology
Economics, Econometrics and Finance
Economics and Econometrics
Energy
Energy (miscellaneous)
Medicine
Medicine (miscellaneous)
PUBLISHER
Elsevier
H-INDEX
144
% International Collaboration
Citable documents
Non-citable documents
Cited documents
Uncited documents
International Journal of Biological Macromolecules
Q1
Economics and Econometrics
best quartile
SJR 2021
1.1
powered by scimagojr.com
Show this widget in your own website
Just copy the code below and paste within your html code:
SCImago Graphica
Explore, visually communicate and make sense of data with our new data visualization tool.
Ads by Google
Send feedback
Why this ad?

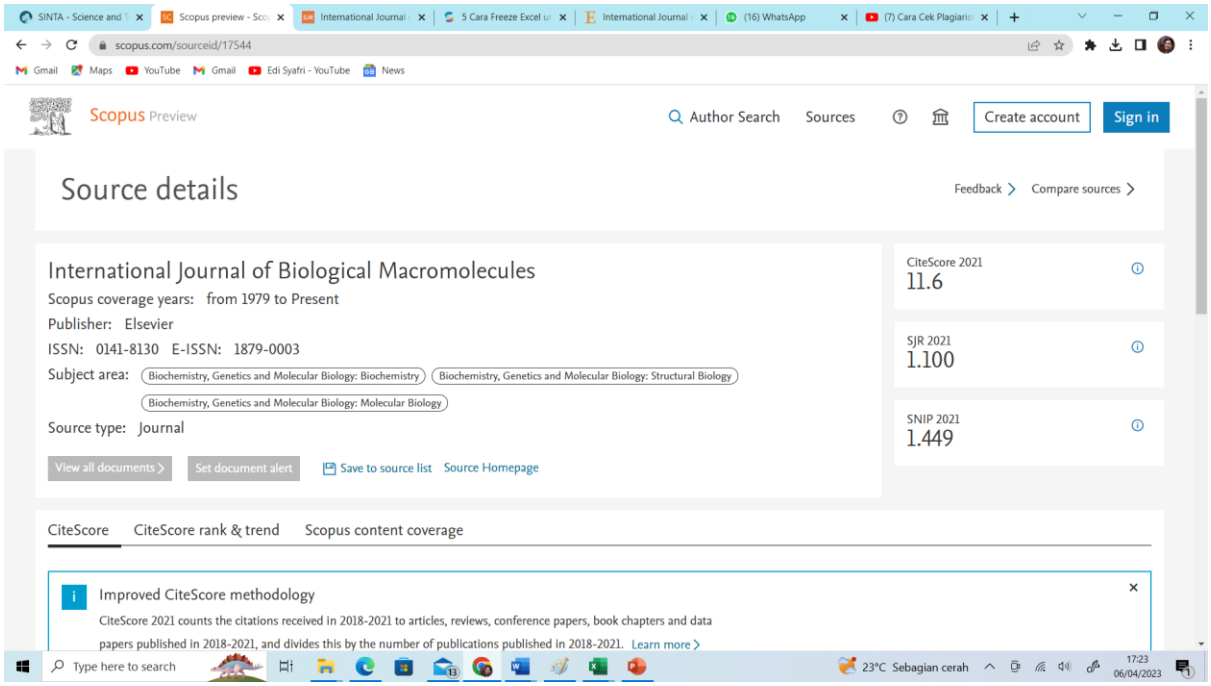

List Of Contents

Volume 154, 1 July 2020, Pages 1419-1425

Research article

Characteristics of sulfated and carboxylated cellulose nanocrystals extracted from *Juncus* plant stems

Zineb Kassab, Edi Syafri, Youssef Tamraoui, Hassan Hannache, ... Mounir El Achaby

Pages 1419-1425

Article preview

☐ select article Alginate beads impregnated with magnetic Chitosan@Zeolite nanocomposite for cationic methylene blue dye removal from aqueous solution

Research articleAbstract only

Alginate beads impregnated with magnetic Chitosan@Zeolite nanocomposite for cationic methylene blue dye removal from aqueous solution

Javad Kazemi, Vahid Javanbakht

Pages 1426-1437

Article preview

☐ select article Sulfated modification, characterization, and potential bioactivities of polysaccharide from the fruiting bodies of Russula virescens

Research articleAbstract only

Sulfated modification, characterization, and potential bioactivities of polysaccharide from the fruiting bodies of *Russula virescens*

Hui Li, Xin Wang, Qian Xiong, Ying Yu, Lincai Peng

Pages 1438-1447

Article preview

select article An insight into the inhibition of fibrillation process verses disaggregation of preformed fibrils of bovine serum albumin by isoprenaline hydrochloride

Research articleAbstract only

An insight into the inhibition of fibrillation process verses disaggregation of preformed fibrils of bovine serum albumin by isoprenaline hydrochloride

Tajalli Ilm Chandel, Mariyam Afghani, Aiman Masroor, Ibrar Ahmad Siddique, ... Rizwan Hasan Khan

Pages 1448-1459

Article preview

select article A novel Hericium erinaceus polysaccharide: Structural characterization and prevention of H₂O₂-induced oxidative damage in GES-1 cells

Research articleAbstract only

A novel *Hericium erinaceus* polysaccharide: Structural characterization and prevention of H_2O_2-induced oxidative damage in GES-1 cells

Bingwu Liao, Chunhui Zhou, Tingting Liu, Yangyan Dai, Huihua Huang

Pages 1460-1470

Article preview

select article Effect of sodium citrate/polyethylene glycol on plasticization and retrogradation of maize starch

Research articleAbstract only

Effect of sodium citrate/polyethylene glycol on plasticization and retrogradation of maize starch

Kang Zhang, Tingbing Su, Fei Cheng, Yi Lin, ... Dacheng Wu

Pages 1471-1477

Article preview

select article Nano-hydroxyapatite incorporated gelatin/zein nanofibrous membranes: Fabrication, characterization and copper adsorption

Research articleAbstract only

Nano-hydroxyapatite incorporated gelatin/zein nanofibrous membranes: Fabrication, characterization and copper adsorption

Lingli Deng, Yang Li, Aiping Zhang, Hui Zhang

Pages 1478-1489

Article preview

select article Immobilization of β-glucosidase by self-catalysis and compared to crosslinking with glutaraldehyde

Research articleAbstract only

Immobilization of β-glucosidase by self-catalysis and compared to crosslinking with glutaraldehyde

Sidra Naseer, Jie Ouyang, Xing Chen, Shujin Pu, ... Chengli Yang

Pages 1490-1495

Article preview

select article Novel polydatin-loaded chitosan nanoparticles for safe and efficient type 2 diabetes therapy: In silico, in vitro and in vivo approaches

Research articleAbstract only

Novel polydatin-loaded chitosan nanoparticles for safe and efficient type 2 diabetes therapy: *In silico, in vitro* and *in vivo* approaches

Adel Abdel-Moneim, Ahmed El-Shahawy, Ahmed Ismail Yousef, Sanaa Mahmoud Abd El-Twab, ... Mohamed Taha

Pages 1496-1504
Article preview
select article Inhibition of Tau amyloid fibril formation by folic acid: In-vitro and theoretical studies
Research articleAbstract only
Inhibition of Tau amyloid fibril formation by folic acid: *In-vitro* and theoretical studies
Samin Ghasemzadeh, Gholam Hossein Riazi
Pages 1505-1516
Article preview
select article Biochemical and functional properties of a new l-amino acid oxidase (LAAO) from Micrurus lemniscatus snake venom
Research articleAbstract only
Biochemical and functional properties of a new L-amino acid oxidase (LAAO) from *Micrurus lemniscatus* snake venom
Thiago Geraldo Soares, Jaqueline Leal dos Santos, Valéria Gonçalves de Alvarenga, Janete Soares Coelho Santos, ... Márcia Helena Borges
Pages 1517-1527
Article preview
select article Synthesis of hemicellulose hydrogels with tunable conductivity and swelling behavior through facile one-pot reaction
Research articleAbstract only
Synthesis of hemicellulose hydrogels with tunable conductivity and swelling behavior through facile one-pot reaction
Jingyun Wen, Jiyou Yang, Wenyi Wang, Mingfei Li, ... Runcang Sun
Pages 1528-1536
Article preview
select article Adsorption of Pb(II) from aqueous solution by polyacrylic acid grafted magnetic chitosan nanocomposite
Research articleAbstract only
Adsorption of Pb(II) from aqueous solution by polyacrylic acid grafted magnetic chitosan nanocomposite
Dalin Hu, Zhenwei Lian, Hongyi Xian, Ran Jiang, ... Xiao–Kun Ouyang
Pages 1537-1547
Article preview
select article Structure and anti-tumor activity of a polysaccharide from Bletilla ochracea Schltr.
Research articleAbstract only
Structure and anti-tumor activity of a polysaccharide from *Bletilla ochracea* Schltr.
Junfeng Niu, Shangping Wang, Bulei Wang, Lijun Chen, ... Zhezhi Wang
Pages 1548-1555
Article preview
select article Structural characterization and immunomodulatory activity of a novel polysaccharide from Pueraria lobata (Willd.) Ohwi root
Research articleAbstract only
Structural characterization and immunomodulatory activity of a novel polysaccharide from *Pueraria lobata* (Willd.) Ohwi root
Zhou Dong, Mengmeng Zhang, Huixian Li, Qiping Zhan, ... Hui Wu
Pages 1556-1564

Article preview

select article Marine waste to a functional biomaterial: Green facile synthesis of modified-β-chitin from Uroteuthis duvauceli pens (gladius)

Research articleAbstract only

Marine waste to a functional biomaterial: Green facile synthesis of modified-β-chitin from *Uroteuthis duvauceli* pens (gladius)

Jolleen Natalie I. Balitaan, Jui-Ming Yeh, Karen S. Santiago

Pages 1565-1575

Article preview

select article Recombinant engineered phage-derived enzybiotic in Pichia pastoris X-33 as whole cell biocatalyst for effective biocontrol of Vibrio parahaemolyticus in aquaculture

Research articleAbstract only

Recombinant engineered phage-derived enzybiotic in *Pichia pastoris* X-33 as whole cell biocatalyst for effective biocontrol of *Vibrio parahaemolyticus* in aquaculture

Ramachandran Srinivasan, Amballa Chaitanyakumar, Parthiban Subramanian, Anbazhagan Mageswari, ... Kodiveri Muthukaliannan Gothandam

Pages 1576-1585

Article preview

select article Improving the catalytic performance of Proteinase K from Parengyodontium album for use in feather degradation

Research articleAbstract only

Improving the catalytic performance of Proteinase K from *Parengyodontium album* for use in feather degradation

Yaxin Ren, Huiying Luo, Huoqing Huang, Nina Hakulinen, ... Tao Tu

Pages 1586-1595

Article preview

select article Metabolic engineering of Pseudomonas mendocina NK-01 for enhanced production of medium-chain-length polyhydroxyalkanoates with enriched content of the dominant monomer

Research articleAbstract only

Metabolic engineering of *Pseudomonas mendocina* NK-01 for enhanced production of medium-chain-length polyhydroxyalkanoates with enriched content of the dominant monomer

Fengjie Zhao, Fanyang He, Xiangsheng Liu, Jie Shi, ... Ruihua Liu

Pages 1596-1605

Article preview

Nanotechnology with Biological Macromolecules

select article Alginate-coated caseinate nanoparticles for doxorubicin delivery: Preparation, characterisation, and in vivo assessment

Research articleAbstract only

Alginate-coated caseinate nanoparticles for doxorubicin delivery: Preparation, characterisation, and *in vivo* assessment

Nihal Saad Elbialy, Noha Mohamed

Pages 114-122

Article preview

select article Preparation and characterization of antibacterial magnetic-/pH-sensitive alginate/Ag/Fe₃O₄ hydrogel beads for controlled drug release

Research articleAbstract only

Preparation and characterization of antibacterial magnetic-/pH-sensitive alginate/Ag/Fe_3O_4 hydrogel beads for controlled drug release

Bahaaldin Rashidzadeh, Ebrahim Shokri, Gholam Reza Mahdavinia, Reza Moradi, ... Shadi Abdi

Pages 134-141

Article preview

☐ select article pH-sensitive natural almond gum hydrocolloid based magnetic nanocomposites for theragnostic applications

Research articleAbstract only

pH-sensitive natural almond gum hydrocolloid based magnetic nanocomposites for theragnostic applications

D. Jaison, Gopalakrishnan Chandrasekaran, M. Mothilal

Pages 256-266

Article preview

☐ select article Carbohydrate and protein based biopolymeric nanoparticles: Current status and biotechnological applications

Review articleAbstract only

Carbohydrate and protein based biopolymeric nanoparticles: Current status and biotechnological applications

Madan L. Verma, B.S. Dhanya, Sukriti, Varsha Rani, ... Rekha Kushwaha

Pages 390-412

Article preview

☐ select article Thermally self-assembled biodegradable poly(casein-g-N-isopropylacrylamide) unimers and their application in drug delivery for cancer therapy

Research articleAbstract only

Thermally self-assembled biodegradable poly(casein-g-N-isopropylacrylamide) unimers and their application in drug delivery for cancer therapy

Julio C. Cuggino, Franco E. Ambrosioni, Matías L. Picchio, Maribel Nicola, ... Luis M. Gugliotta

Pages 446-455

Article preview

☐ select article pH-induced structural transition during complexation and precipitation of sodium caseinate and ε-Poly-l-lysine

Research articleAbstract only

pH-induced structural transition during complexation and precipitation of sodium caseinate and *ε*-Poly-L-lysine

Liang Guo, Yaqian Fang, Zhipeng Shao, Sheng Fang, ... Yuecheng Meng

Pages 644-653

Article preview

☐ select article Dual catalytic DNA circuit-induced gold nanoparticle aggregation: An enzyme-free and colorimetric strategy for amplified detection of nucleic acids

Research articleAbstract only

Dual catalytic DNA circuit-induced gold nanoparticle aggregation: An enzyme-free and colorimetric strategy for amplified detection of nucleic acids

Hadi Ravan, Mojdeh Amandadi, Mehdi Hassanshahian, Shahram Pourseyedi

Pages 896-903

Article preview

☐ select article Cellulose from sources to nanocellulose and an overview of synthesis and properties of nanocellulose/zinc oxide nanocomposite materials

Review articleAbstract only

Cellulose from sources to nanocellulose and an overview of synthesis and properties of nanocellulose/zinc oxide nanocomposite materials

Amjad Farooq, Mohammed Kayes Patoary, Meiling Zhang, Hassan Mussana, ... Lifang Liu

Pages 1050-1073

International Journal of Biological Macromolecules 154 (2020) 1419–1425

Contents lists available at ScienceDirect

International Journal of Biological Macromolecules

journal homepage: www.elsevier.com/locate/ijbiomac

Characteristics of sulfated and carboxylated cellulose nanocrystals extracted from *Juncus* plant stems

Zineb Kassab [a,b], Edi Syafri [c], Youssef Tamraoui [a], Hassan Hannache [a,b], Abou El Kacem Qaiss [d], Mounir El Achaby [a,*]

[a] Materials Science and Nanoengineering Department (MSN), Mohammed VI Polytechnic University (UM6P), Lot 660 – Hay Moulay Rachid, 43150 Benguerir, Morocco
[b] Laboratoire d'Ingénierie et Matériaux (LIMAT), Faculté des Sciences Ben M'sik, Université Hassan II de Casablanca, B.P.7955 Casablanca, Morocco
[c] Department of Agricultural Technology, Agricultural Polytechnic, Payakumbuh, West Sumatra 26271, Indonesia
[d] Composites and Nanocomposites Center (CNC), Moroccan Foundation for Advanced Science, Innovation and Research (MAScIR), Rabat Design, Rue Mohamed El Jazouli, Madinat El Irfane, 10100 Rabat, Morocco

ARTICLE INFO

Article history:
Received 1 August 2019
Received in revised form 25 October 2019
Accepted 5 November 2019
Available online 14 November 2019

Keywords:
Juncus plant stems
Acid hydrolysis
Cellulose nanocrystals

ABSTRACT

In this study, sulfated and carboxylated cellulose nanocrystals (CNC) have been produced from newly identified cellulose-rich bio-sourced material, namely *Juncus* plant. The *Juncus* plant stems were firstly subjected to chemical treatments to produce purified cellulose microfibers (CMF) with an average diameter of 3.5 μm and yield of 36%. By subjecting CMF to sulfuric and citric/hydrochloric mixture acids hydrolysis, sulfated CNC (S-CNC) and carboxylated CNC (C-CNC) have been produced with a diameter of 7.3 ± 2.2 and 6.1 ± 2.8 nm, and a length of 431 ± 94 and 352 ± 79 nm, respectively. These newly extracted S-CNC and C-CNC exhibited a crystallinity of 81% and 83% with cellulose *I* structure and showed high thermal stability (>200 °C). Herein, this newly identified *Juncus* plant, which is a naturally-derived source, could be used as a valuable alternative to conventional sources such as wood and cotton for nanocellulose production. We speculate that the determined high thermal stability, the large aspect ratio and high crystallinity will allow the use of the extracted CNC as nano-reinforcing agents in polymers that require processing temperatures of up to 200 °C. Owing to their surface functionalities (sulfated or carboxylated surface groups), the here produced CNC could be used as nano-additives or nano-reinforcing agents for water-soluble bio-polymers in order to produce bio-nanocomposites by solvent casting techniques.

1. Introduction

The identification of new renewable sources for the production of biodegradable naturally-derived nanomaterials has steadily increased in recent years [1,2]. There are various unexplored valuable cellulose-rich materials found in nature and not yet valorized for the production of cellulose derivatives such as cellulose microfibers (CMF), cellulose nanofibrils (CNF) and cellulose nanocrystals (CNC). These non-conventional sources could be used as an important alternative to conventional sources such as wood and cotton [3]. In this context, various natural fibers, agricultural by-products, and marine biomass have been recently identified as renewable sources for cellulose derivatives production [3–14]. Among such underutilized renewable sources, *Juncus* plant (*Juncus* effusus L, rush or smmar in Arabic) is one of the naturally-derived materials that is rich in cellulose product and widely abundant in nature, especially in African countries [15,16]. It is a widespread plant belonging to *Juncaceae* family with about 200 species, growing in different environmental conditions, especially in wet places (lakes, rivers, ponds, mountain, etc.). The *Juncus* plant is in the form of a tuft of grass consisting of hollow cylindrical rods of about 1 m in height and 4–8 mm in diameter containing a white spongy material. Generally, these plants are harvested and processed into woven textiles such as baskets and fiber mat [17]. In addition, researchers previously revealed that fibers from Juncus plant have a good potential as polymer reinforcing fillers [15–17]. Importantly, the high content of cellulose in *Juncus* plant (40 wt%) [16], make it a very interesting bio-sourced raw material for the production of cellulose derivatives such as CMF and CNC.

To produce pure cellulose fibers from cellulose-rich renewable sources, the researchers used chemical methods such as alkalization and bleaching treatments [1,2,18]. The role of two treatments above is the removal of non-cellulosic components presented in

* Corresponding author.
E-mail address: mounir.elachaby@um6p.ma (M. El Achaby).

https://doi.org/10.1016/j.ijbiomac.2019.11.023
0141-8130/

the raw matter, namely lignin, hemicellulose and other extractive substances, leading in the production of purified cellulose fibers [1,2]. Once pure cellulose is extracted from lignocellulosic materials, other derivatives could be obtained, through etherification, esterification, oxidation and nitration reactions, such as hydroxyethyl cellulose, ethyl cellulose, hydroxypropyl cellulose, cellulose acetate, cellulose nitrate, carboxymethyl cellulose (CMC) and others [19–21]. On the other hand, by subjecting purified cellulose fibers to acid hydrolysis or mechanical treatment (ultrasonic cell crusher, high shear homogenizer and centrifugation), nanocelluloses could be produced such as CNC and CNF [4,22]. The unique characteristics of nanocelluloses make them potential natural nanomaterials for many applications [3,23,24].

The use of acid hydrolysis process to breakdown the purified cellulose fibers is the most effective method, where the cellulose fibers are subjected to concentrated acid to hydrolyze the amorphous domains of the cellulose chains and leave the crystalline domains unaltered, named CNC [23]. Various acids have been used for this purpose, resulting in CNC with different structural, morphological and thermal properties and controlled surface functionality [25,26]. In this context, the sulfuric acid has been extensively used for CNC extraction; however, hydrochloric, phosphoric and hydrobromic acids have also been reported for such purpose [26–28]. The sulfuric acid hydrolysis is a simple process and it requires shorter reaction time than other processes [29]. Additionally, this process produces CNC with inserted anionic sulfate groups on its surface, high crystallinity and good colloidal stability in water [27]. Recently, the use of a mixture of citric and hydrochloric acids for isolation of CNC with carboxylated surface functionality was reported [25]. Generally, the physico-chemical properties of cellulose and its derivatives such CNC and MCC (microcrystalline cellulose) are strongly related to the nature of the bio-sourced raw materials and the hydrolysis conditions such as acid type, reaction time and temperature and acid concentration [30–32]. Recently, Tarchoun et al. reported the isolation of MCC by various acids namely hydrochloric acid, nitric acid, sulfuric acid, and their mixtures [32]. They found that the type of the hydrolysis acidic medium could affect the properties of the produced MCC, especially the morphology and the crystallinity index.

The novelty of this work is the conversion of the newly identified *Juncus* plant stems into purified micro-sized cellulose fibers and CNC with different characteristics and surface functionalities. The use of sulfuric acid and citric/hydrochloric mixture acid hydrolysis processes resulted in the isolation of sulfated CNC (S-CNC) and carboxylated CNC (C-CNC), respectively. The as-produced S-CNC and C-CNC were characterized in terms of their morphologies, dimensions, structure, crystallinity and thermal stability.

2. Materials and methods

2.1. Materials

The raw *Juncus* stems used in this work was collected from the province of Settat, Morocco. The as-received raw Juncus stems were cut into 2–4 cm small fibers, and then they were ground using a home coffee mill. Analytical grade chemicals used for the treatment of raw *Juncus* stems and the extraction of cellulosic materials were purchased from Sigma–Aldrich.

2.2. Isolation of purified cellulose microfibers (CMF)

Raw ground *Juncus* stems were washed with distilled water for 1 h at 60 °C under mechanical stirring. The prewashed stems were treated two times with 4 wt% NaOH solution at 80 °C for 2 h under stirring. The alkali-treated *Juncus* fibers were bleached using a solution made up of equal parts (v:v) of acetate buffer (27 g NaOH and 75 mL glacial acetic acid, diluted to 1 L of distilled water) and aqueous sodium chlorite (1.7 wt% $NaClO_2$ in water). This treatment was done three times for 2 h at 80 °C, resulting in cellulose microfibers (CMF) **(**Fig. 1**).**

2.3. Extraction of S-CNC

S-CNC were extracted by subjecting the as-extracted CMF to sulfuric acid hydrolysis [4]. For that, CMF were added to a preheated sulfuric acid solution (64 wt%) (9 M) at 50 °C under mechanical stirring for 30 min. Then, the mixture was diluted with ice cubes to stop the reaction. The obtained mixture was washed by successive centrifugations at 12,000 rpm at 15 °C for 15 min at each step. The obtained mixture was dialyzed against distilled water until it reached a neutral pH. Afterward, the obtained CNC aqueous suspension was homogenized using a probe-type ultrasonic homogenizer for 5 min in an ice bath. Photograph of the obtained freeze-dried S-CNC is shown in Fig. 1.

2.4. Extraction of C-CNC

C-CNC were extracted by subjecting the as-extracted CMF to citric acid/hydrochloric acid mixture hydrolysis [25]. In this process, the CMF were added to a preheated acid solution made from 90% citric acid (3 M) and 10% hydrochloric acid (6 M) (v/v). The reaction was performed at 80 °C for 4 h under mechanical stirring. Subsequently, after cooling to room temperature, the resultant suspension was repeatedly washed several times using successive centrifugations at 12,000 rpm at 15 °C for 15 min at each step, then dialyzed against distilled water until it reached a neutral pH. The resulted C-CNC suspension was sonicated for 15 min using a probe-type ultrasonic homogenizer. Photograph of the obtained freeze-dried C-CNC is shown in Fig. 1.

2.5. Materials characterization

The fibers morphology was observed by field-emission scanning electron microscopy (SEM, HIROX SH 4000M). The samples were first coated by a thin conductive carbon layer to help improve SEM images. Atomic force microscopy (AFM) (Dimension ICON, Bruker) instrument was used to characterize the dimension and morphological of S-CNC and C-CNC. The CNC suspension (0.01 wt %) was sonicated by ultrasonic bath for 15 min and dispersed on to mica sheet for observation. The dimensions of CNC were directly analyzed by using Veeco Data Analysis Software (NanoScope® Version 8.0 software, Bruker). X-Ray diffraction (XRD) measurement was done by D2 PHASER diffractometer using a CuK ($\lambda = 1.54$, 40 kV, 40 mA) in the range of $2\theta = 5–50°$ with a scanning rate of 2°/min. The *CrI* of all studied sample was measured by Segal equation [33]:

$$C_rI = \frac{I_{200} - I_{am}}{I_{200}} \times 100$$

where I_{200} is maximum peak intensity at 200-lattice plane (crystalline area), and I_{am} is the peak at $2\theta = 18°$ (amorphous area) [33].

Fourier transform-infrared (FTIR) spectroscopy was performed on a Perkin-Elmer Spectrum 2000 FTIR apparatus equipped with attenuated total reflection (ATR) accessory. The FTIR spectra were recorded in 4000–600 cm^{-1} range with a resolution of 4 cm^{-1} and an accumulation of 16 scans. The thermal stability of samples was evaluated by thermogravimetric analysis (TGA, Discovery TGA from TA instruments). The weight of samples tested was 5–10 mg. The samples were heated from room temperature to 700 °C under nitrogen atmosphere with heating rate of 10 °C/min.

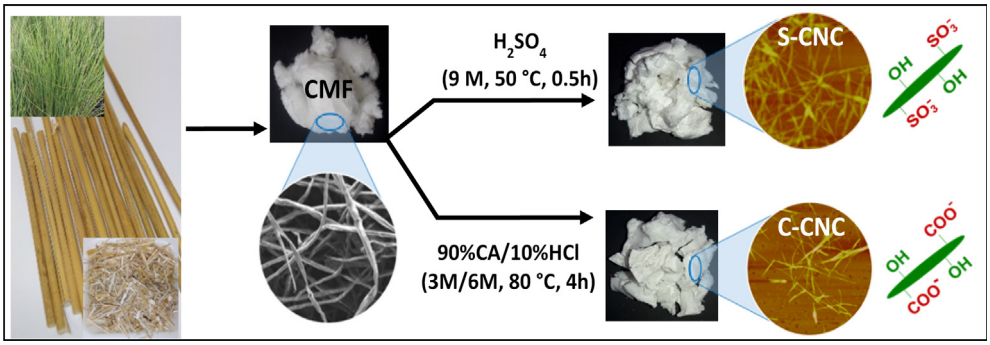

Fig. 1. Overall steps for extraction of CMF and CNC (S-CNC and C-CNC) from raw *Juncus* stems.

3. Results and discussion

3.1. Extraction processes and morphological analysis

Fig. 1 displays the overall steps of the used extraction process and the physical aspect of each material. Before producing CNC (S-CNC and C-CNC), raw *Juncus* stems were transformed into purified CMF *via* alkali and bleaching treatments with a yield of 36%. It is well known that the alkali and bleaching treatments are conventional processes usually applied to purify and remove the non-cellulosic compounds (lignin, hemicellulose, protein and other impurities) from raw finely-ground lignocellulosic materials, leading to the extraction of pure cellulosic fibers [4,18,34–36]. The physico-chemical characteristics of such extracted pure cellulosic fibers are dependent to the source of cellulose and to the experimental conditions used such as the concentration of the alkaline and bleaching solutions, reaction temperature and time [4,35,37,38]. Herein, it was found that the as-extracted CMF from *Juncus* stems exhibited an average microfibers diameter of about 3.5 μm and the obtained microfibers are clearly separated from each other, as observed by SEM analysis (Fig. 2b and c). These microfibers were cemented and connected by lignin and hemicellulose in raw *Juncus* stems, giving a compact structure to the raw stems, as clearly shown in Fig. 2a. The obtaining of individual microfibers is mainly due to the defibrillation of the *Juncus* stems by chemical treatments, which lead to the removal of lignin and hemicellulose molecules bound firmly to CMF [1,18]. This finding suggests that *Juncus* plant is a suitable cellulose-rich source for *CMF* production with the microsized diameter and excellent structural and thermal properties (see below).

Once CMF are obtained, sulfuric acid hydrolysis and citric/hydrochloric mixture hydrolysis were separately applied to solubilize the amorphous parts of CMF, leaving the crystalline parts unaltered, which are identified as S-CNC and C-CNC (Fig. 3). The as-isolated S-CNC and C-CNC showed a gel-like suspension after ultrasonic homogenization process, as illustrated in Fig. 3, which is typical behavior of acid hydrolyzed CNC [18,25,26]. It has been reported that CNC produced with sulfuric acid or citric/hydrochloric mixture acid can be completely suspended at the individual nanocrystal level in aqueous solution by electrostatic repulsion, which are due to the insertion of negatively charged groups on the surface of CNC during acid hydrolysis [4,25,26,39,40]. These negatively charged groups consist of sulfate groups (SO_3^-) in the case of using sulfuric acid hydrolysis and carboxylate groups(COO^-)in the case of using citric/hydrochloric mixture acid hydrolysis. It has been reported that the use of sulfuric acid hydrolysis of cellulose induced a sulfate half-ester reaction between sulfuric acid and cellulose surface, which led to the occurrence of sulfate half-ester groups on the surface of CNC [25,28,41]. While the carboxylate groups can be formed by esterification reaction

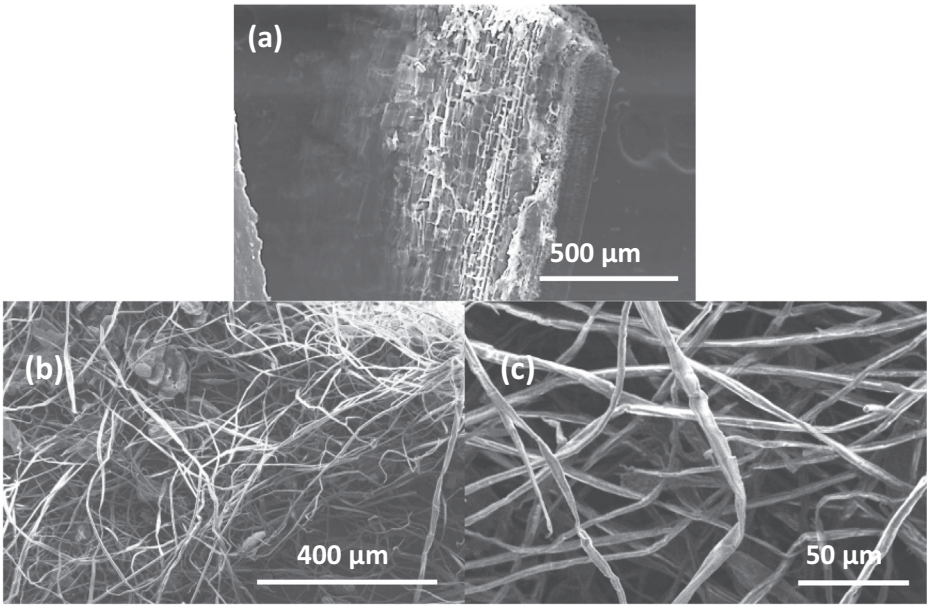

Fig.2. SEM images of (a) raw *Juncus* stems (R-Junc) and (b and c) CMF.

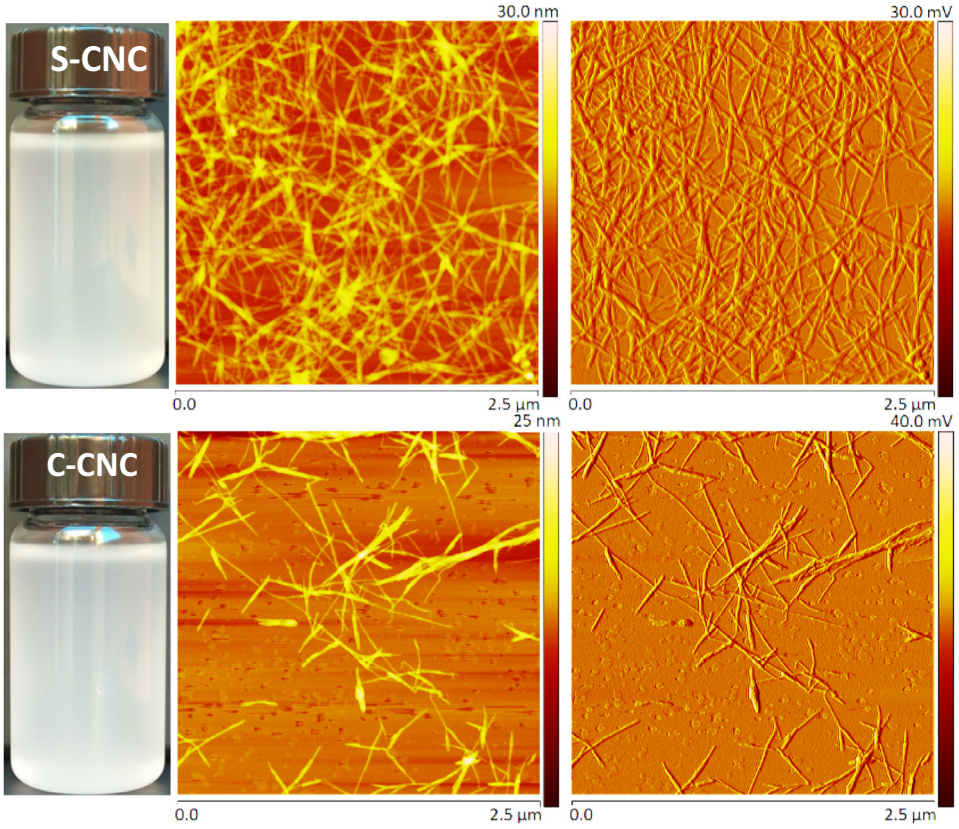

Fig.3. Aqueous suspensions and AFM images of S-CNC (Top) and C-CNC (bottom).

between the hydroxyl groups of cellulose and the carboxyl groups of citric acid, leading into carboxylated CNC (C-CNC) [25].

Fig. 3 shows the AFM images of both extracted CNC (S-CNC and C-CNC), which confirmed the successful isolation of individual nanocrystals after acid hydrolysis process using sulfuric acid and citric/hydrochloric mixture acid hydrolysis process. The AFM images showed that the extracted CNC exhibited a needle-like shape, which is the common shape observed for CNC extracted by acid hydrolysis process [4,34,35]. The average diameter and length of S-CNC was measured at 7.3 ± 2.2 and 431 ± 94 nm (Table 1), respectively, giving rise to an aspect ratio of 59. Comparatively, the measured aspect ratio of S-CNC is higher than that determined for sulfuric acid hydrolysed CNC derived from other new identified sources such as vine shoots (32), pineapple crown waste (6.3) [7], pistachio shells (16) [8], rice and coffee husks (10–20) [9], barely straw (19) [10], acacia bark (11.5–18.6) [11], wheat bran (20–32) [12] and industrial waste cotton (40) [13]. However, it is found to be comparable to that of CNC extracted from other sources such as sugarcane bagasse (55) [14], Sunflower oil cake (65) [5], red algae waste (57) [4], alfa fibers (66) [18], spruce bark (63) [6].

As presented in Fig. 3, the carboxylation treatment showed a separated dispersion of C-CNC with an average diameter and length of 6.1 ± 2.8 and 352 ± 79 nm (Table 1), respectively, resulting in an aspect ratio of 57, which is comparable to that measured for S-CNC (59). It is worth noting that the extraction of C-CNC was carried out using the same process firstly described by *Yu et al.* [25], who extracted C-CNC from commercial microcrystalline cellulose (MCC) *via* a mixture of citric/hydrochloric acids with optimized experimental conditions. Herein, it was found that the measured aspect ratio of C-CNC from *Juncus* stems is very higher than that measured for C-CNC obtained from MCC (13.5) [25], suggesting that the purified cellulose from *Juncus* stems is very interesting source for the production of C-CNC with relatively high aspect ratio.

Remarkably, the smaller diameter and length of C-CNC compared to S-CNC may be due to the strong acidity level of citric/hydrochloric mixture acid that can severely break the amorphous domains of native cellulose, resulting in smaller dimensions. This finding suggests that the as-produced CMF from *Juncus* stems are suitable for the production of CNC with uniform shape, nanometric, high aspect ratio and functionalized surface.

Table 1
Structural and morphological properties of the extracted CNC (S-CNC and C-CNC).

Sample	XRD		AFM		TGA/DTG	
	D (nm)	*L* (nm)	*CrI* (%)	T_{onset} (°C)	T_{max1} (°C)	*R* at 600 °C
R-Junc	–	–	43	189	322	25
CMF	–	–	72	230	356	10
S-CNC	7.3 ± 2.2	431 ± 94	81	221	332	32
C-CNC	6.1 ± 2.8	352 ± 79	83	231	347	17

3.2. Infrared spectroscopy analysis

Fig. 4 illustrates the FTIR spectra of raw *Juncus* stems, CMF, S-CNC and C-CNC. All the samples show the characteristic peaks of cellulose molecules. The region between 3500 and 3000 cm^{-1} is mainly originated from *OH* groups, while the peaks at around 2900 cm^{-1} arise from the *C—H* symmetrical stretching (Fig. 4a) [42]. From Fig. 4b, the band at 1733 cm^{-1} observed only in raw *Juncus* stems sample is assigned to the C=O stretching vibration of the carbonyl and acetyl groups in the xylan component of hemicelluloses [10,32,43]. Furthermore, the bands at 1515 cm^{-1} and 1230 cm^{-1} in the spectrum of raw *Juncus* stems sample are attributed to the C=C stretching from aromatic hydrocarbons of lignin and the stretching vibration mode of the acyl oxygen CO-OR associated with the hemicelluloses, respectively [43–45]. Importantly, these peaks were not observed in the CMF and CNC (S-CNC and C-CNC) spectra, confirming the total removal of lignin and hemicellulose molecules after the applied chemical treatment [1,2,32,43].

Furthermore, it is possible to see that no substantial difference can be observed between the FTIR spectra of the extracted CNC and that of CMF, indicating that the chemical structure of the cellulose was not altered during acid hydrolysis process using the two selected acid media. This finding is in accordance with previously reported studies [32]. It is worth noting that sulfate and carboxylate groups were introduced on the surface of S-CNC [18] and C-CNC [25] during the sulfuric and citric/hydrochloric acid hydrolysis, respectively. The band relative to sulfate negatively charged groups is generally observed at 1202 cm^{-1} [18], which is overlapped with the main characteristics of cellulose molecules in the FTIR spectrum of S-CNC sample, while a small new band at 1725 cm^{-1} can be observed in the spectrum of C-CNC (Fig. 4b), which is associated to carboxylate groups (COO^{-}) inserted on the surface of C-CNC, which were formed by esterification reaction between the hydroxyl groups of cellulose and the carboxyl groups of citric acid, as proposed by *Yu et al.* [25]. Consequently, the FTIR results confirmed the successful extraction of pure CMF and surface functionalized CNC from the newly identified *Juncus* plant stems.

3.3. Crystalline structure

Fig. 5 showed XRD characteristics of raw *Juncus* stems, CMF, S-CNC and C-CNC. All samples showed four major reflection peaks appeared at $2\theta = 14.9°$, 16.1°, 22.2° and 34.4°, corresponding to $1\bar{1}0$,110, 200, and 004 typical reflection planes of cellulose *I* structure [18]. This result confirmed that the raw *Juncus* plant stems could be considered as lignocellulosic material. It is also confirmed that the polymorphism of cellulose *I* structure, originally presents in the raw *Juncus* stems, was not altered after the successive chemical treatments applied at different stages, including alkali and bleaching treatments as well as acid hydrolysis processes.

The crystallinity index (*CrI*) values measured for all studied samples are listed in Table 1. The *CrI* was found to be about 43%, 72%, 81%, and 83% for raw *Juncus* stems, CMF, S-CNC and C-CNC samples, respectively. The increasing of *CrI* from raw *Juncus* stems to CMF is associated with the total removal of amorphous non-cellulosic compounds such as lignin, hemicellulose and others. The increased *CrI* observed for S-CNC and C-CNC, compared to CMF, was expected since the role of the applied acid hydrolysis is to solubilize the amorphous regions of cellulose, leaving the crystalline domains unaltered, as observed by AFM images (Fig. 3). The obtained *CrI* for S-CNC and C-CNC is comparable to that reported for CNC extracted from other sources using acid hydrolysis process [4,6,18,25,26,34,45]. This finding suggests that the raw *Juncus* stems are very interesting naturally-derived material for obtaining CNC with high crystallinity, which is very important property for the application of CNC, especially as nano-reinforcing agents for polymer nanocomposites development.

3.4. Thermal degradation behavior

TGA and DTG of raw *Juncus* stems and the extracted CMF, S-CNC and C-CNC are displayed in Fig. 6a and b, respectively, and the thermal parameters such as the onset temperature (T_{onset}) and the maximum degradation temperature (T_{max}) are listed in Table 1. The raw *Juncus* stems showed the lower thermal stability regarding its extracted parts (CMF and CNC). The T_{onset} and T_{max} of raw *Juncus* plant were measured at 189 and 322 °C, respectively, which are 41 and 34 °C lower than those observed for CMF (230 and 356 °C). This finding is due to the removal of non-cellulosic compounds (lignin and hemicellulose) that are characterized by low thermal stability [10,32,33,45–47].

The extracted CNC (S-CNC and C-CNC) showed very good thermal stability, especially the sulfuric acid hydrolyzed CNC (S-CNC),

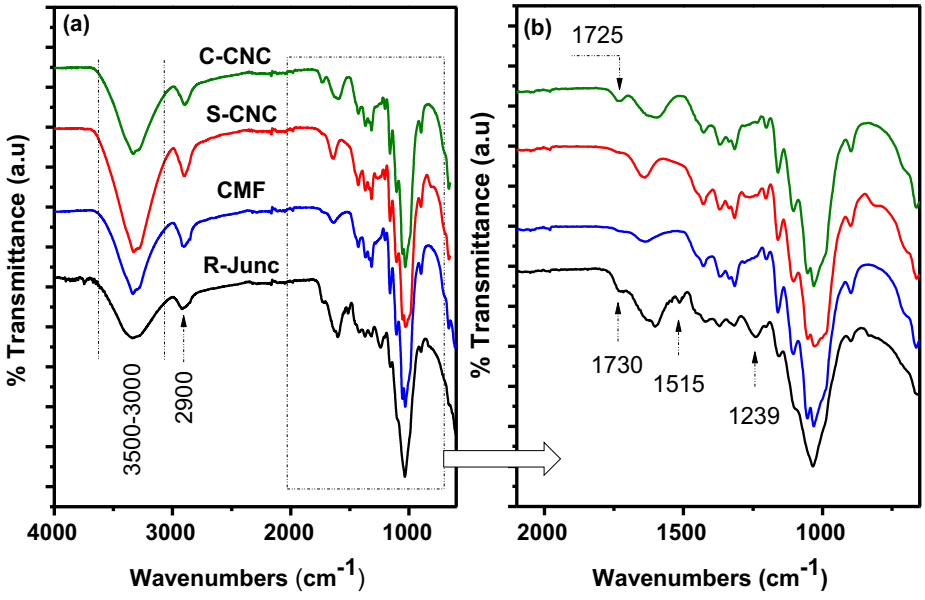

Fig. 4. FTIR spectra of raw *Juncus* stems (R-Junc), CMF and CNC (S-CNC and C-CNC).

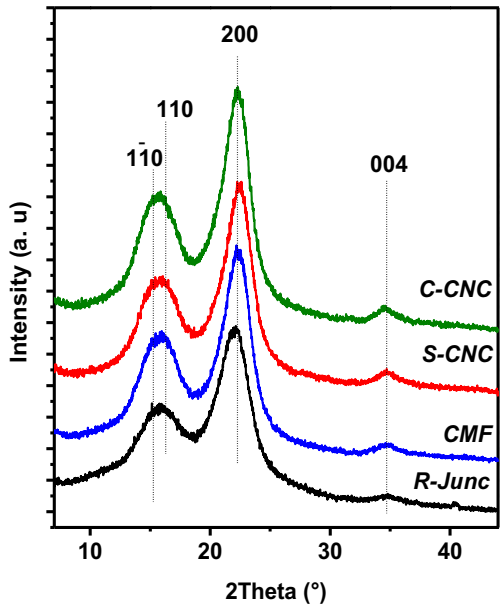

Fig.5. XRD patterns of raw *Juncus* stems (R-Junc), CMF and CNC (S-CNC and C-CNC).

that are generally suffer from its limited thermal stability. Herein, the T_{onset} determined for S-CNC was found to be 221 °C (with a T_{max} of 332 °C), which is higher than that earlier reported in the literature for S-CNC extracted from other sources [4,5,14,18,35,36,48,49]. This finding suggests that the native cellulose (CMF) extracted from *Juncus* stems source is suitable for extracting thermally stable CNC by sulfuric acid, which represents the effective acid generally used for this purpose. On the other hand, the thermal stability of C-CNC (T_{onset} of 231 °C) is comparable to that observed for CMF (T_{onset} of 230 °C) and slightly higher than that measured for S-CNC (T_{onset} of 221 °C), suggesting that the thermal stability of acid-hydrolysed CNC are influenced by the experimental extraction conditions, as previously reported in the literature [4,26]. In contrast, the obtained thermal stability of C-CNC is lower than that reported by *Yu et al.* for C-CNC extracted from microcrystalline cellulose using the same extraction process [25], who found a T_{onset} and T_{max} of 283 °C and 353 °C, respectively, which are 52 °C and 6 °C higher than those measured in this work. This finding suggests that the level of thermal stability CNC is strongly related to the source of cellulose [10].

From the TGA curves and the values listed in Table 1, it is possible to see that the studied samples showed a different behaviour concerning the char residue at 600 °C. Indeed, the thermal decomposition of CMF sample resulted in reduced char residue (10%) as compared to raw *Juncus* stems (25%), which is probably due to the absence of the charred residue that can be generated from the degradation of lignin and hemicelluloses [34,45]. However, these molecules have been totally removed by the bleaching treatment, which confirms the low content of char residue for CMF sample. Moreover, S-CNC showed a relatively high char residue (32%) as compared to the CMF sample (10%), due to the insertion of sulfate groups that act as flame-retardants [45]. The higher char residue produced by S-CNC as compared to C-CNC (17%) is probably due to the higher surface functionalization and the lower temperature required for degradation of S-CNC.

4. Conclusions

Cellulose microfibers (CMF) and cellulose nanocrystals (CNC) have been successfully produced from *Juncus* plant stems. This later was identified for the first time as naturally-derived lignocellulosic material for the extraction of micro- and nano-cellulose fibers. Conventional purification processes such as alkaline and bleaching treatments were applied to raw *Juncus* stems, resulting in the production of pure CMF with an average microfibers diameter of 3.5 μm and a crystallinity of 72%. By subjecting CMF to sulfuric acid and citric/hydrochloric mixture acid hydrolysis, sulfated CNC (S-CNC) and carboxylated CNC (C-CNC) were separately obtained with different characteristics. Morphologically, the as-produced S-CNC and C-CNC exhibited a needle-like shape with an average diameter of 7.3 ± 2.2 and 6.1 ± 2.8 nm, and an average length of 431 ± 94 and 352 ± 79 nm, giving rise to an aspect ratio of 59 and 57, respectively. The crystallinity of S-CNC and C-CNC was measured as 81% and 83%, respectively. The thermal stability of the as-extracted S-CNC and C-CNC was found to be higher than that earlier reported for CNC from other sources extracted by sulfuric acid hydrolysis process, which is the largely employed technique, but the resulted CNC usually suffer from limited thermal stability. Through this study, we have demonstrated a possible strategy to give an added value to raw *Juncus* plant, which is rich in cellulose, inexpensive and renewable source. The extraction of

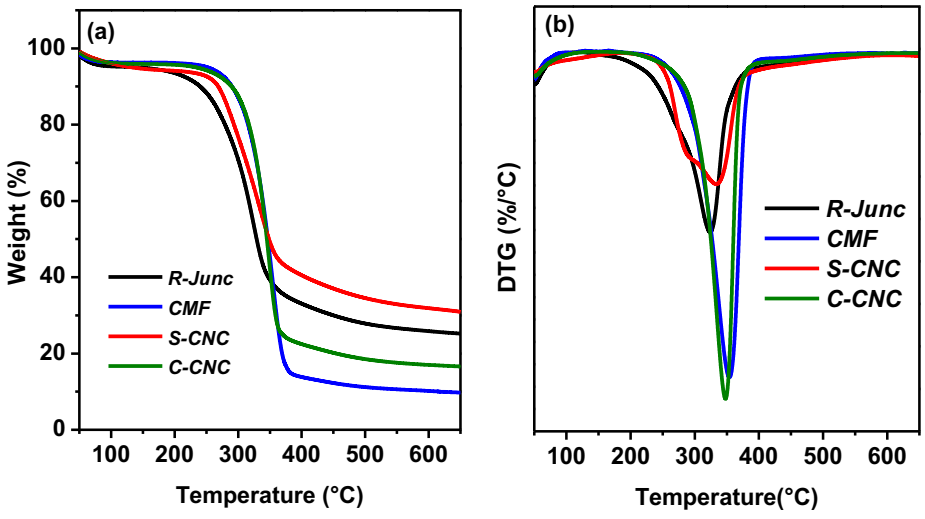

Fig.6. (a) TGA and (b) DTG curves of raw *Juncus* stems (R-Junc), CMF and CNC (S-CNC and C-CNC).

CNC with excellent properties from this newly identified *Juncus* plant could be used as potential nano-reinforcing agents for polymer nanocomposites manufacturing using melt processing techniques for a temperature below to 200 °C and for other functional applications.

Acknowledgement

The financial assistance of the Office Chérifien des Phosphates (OCP S.A.) in the Moroccan Kingdom toward this research is hereby acknowledged.

References

[1] J. Prasad Reddy, J.W. Rhim, Isolation and characterization of cellulose nanocrystals from garlic skin, Mater. Lett. 129 (2014) 20–23.
[2] A.N. Frone, I. Chiulan, D.M. Panaitescu, C.A. Nicolae, M. Ghiurea, A.-M., Galan (former Popescu), Isolation of cellulose nanocrystals from plum seed shells, structural and morphological characterization, Mater. Lett. 194 (2017) 160–163.
[3] D. Trache, M.H. Hussin, M.K.M. Haafiz, V.K. Thakur, Recent progress in cellulose nanocrystals: sources and production, Nanoscale 9 (2017) 1763–1786.
[4] M. El Achaby, Z. Kassab, A. Aboulkas, C. Gaillard, A. Barakat, Reuse of red algae waste for the production of cellulose nanocrystals and its application in polymer nanocomposites, Int. J. Biol. Macromol. 106 (2018) 681–691.
[5] Z. Kassab, M. El Achaby, Y. Tamraoui, H. Sehaqui, R. Bouhfid, A.E.K. Qaiss, Sunflower oil cake-derived cellulose nanocrystals: extraction, physico-chemical characteristics and potential application, Int. J. Biol. Macromol. 136 (2019) 241–252.
[6] M. Le Normand, R. Moriana, M. Ek, Isolation and characterization of cellulose nanocrystals from spruce bark in a biorefinery perspective, Carbohydr. Polym. 111 (2014) 979–987.
[7] K.S. Prado, M.A.S. Spinacé, Isolation and characterization of cellulose nanocrystals from pineapple crown waste and their potential uses, Int. J. Biol. Macromol. 122 (2019) 410–416.
[8] J. Marett, A. Aning, E.J. Foster, The isolation of cellulose nanocrystals from pistachio shells via acid hydrolysis, Ind. Crops Prod. 109 (2017) 869–874.
[9] S. Collazo-Bigliardi, R. Ortega-Toro, A. Chiralt Boix, Isolation and characterisation of microcrystalline cellulose and cellulose nanocrystals from coffee husk and comparative study with rice husk, Carbohydr. Polym. 191 (2018) 205–215.
[10] A.A. Oun, J.W. Rhim, Isolation of cellulose nanocrystals from grain straws and their use for the preparation of carboxymethyl cellulose-based nanocomposite films, Carbohydr. Polym. 150 (2016) 187–200.
[11] T. Taflick, L.A. Schwendler, S.M.L. Rosa, C.I.D. Bica, S.M.B. Nachtigall, Cellulose nanocrystals from acacia bark–Influence of solvent extraction, Int. J. Biol. Macromol. 101 (2017) 553–561.
[12] Y. Xiao, Y. Liu, X. Wang, M. Li, H. Lei, H. Xu, Cellulose nanocrystals prepared from wheat bran: characterization and cytotoxicity assessment, Int. J. Biol. Macromol. 140 (2019) 225–233.
[13] S. Thambiraj, D. Ravi Shankaran, Preparation and physicochemical characterization of cellulose nanocrystals from industrial waste cotton, Appl. Surf. Sci. 412 (2017) 405–416.
[14] Z. Kassab, F. Aziz, H. Hannache, H. Ben Youcef, M. El Achaby, Improved mechanical properties of k-carrageenan-based nanocomposite films reinforced with cellulose nanocrystals, Int. J. Biol. Macromol. 123 (2019) 1248–1256.
[15] M. Maache, A. Bezazi, S. Amroune, F. Scarpa, A. Dufresne, Characterization of a novel natural cellulosic fiber from Juncus effusus, Carbohydr. Polym. 171 (2017) 163–172.
[16] H. Naili, A. Jelidi, O. Limam, R. Khiari, Extraction process optimization of Juncus plant fibers for its use in a green composite, Ind. Crop. Prod. 107 (2017) 172–183.
[17] S. Hamza, H. Saad, B. Charrier, N. Ayed, F. Charrier-El Bouhtoury, Physico-chemical characterization of Tunisian plant fibers and its utilization as reinforcement for plaster based composites, Ind. Crops Prod. 49 (2013) 357–365.
[18] M. El Achaby, Z. Kassab, A. Barakat, A. Aboulkas, Alfa fibers as viable sustainable source for cellulose nanocrystals extraction: application for improving the tensile properties of biopolymer nanocomposite films, Ind. Crops Prod. 112 (2018) 499–510.
[19] F. Joubert, O.M. Musa, D.R.W. Hodgson, N.R. Cameron, The preparation of graft copolymers of cellulose and cellulose derivatives using ATRP under homogeneous reaction conditions, Chem. Soc. Rev. 43 (2014) 7217–7235.
[20] D. Trache, K. Khimeche, A. Mezroua, M. Benziane, Physicochemical properties of microcrystalline nitrocellulose from Alfa grass fibres and its thermal stability, J. Therm. Anal. Calorim. 124 (2016) 1485–1496.
[21] M.-C. Li, Q. Wu, K. Song, H.N. Cheng, S. Suzuki, T. Lei, Chitin nanofibers as reinforcing and antimicrobial agents in carboxymethyl cellulose films: influence of partial deacetylation, ACS Sustain. Chem. Eng. 4 (2016) 4385–4395.
[22] N.-M. Park, S. Choi, J.E. Oh, D. Youn Hwang, Facile extraction of cellulose nanocrystals, Carbohydr. Polym. (2019), https://doi.org/10.1016/J.CARBPOL.2019.115114.
[23] N. Grishkewich, N. Mohammed, J. Tang, K.C. Tam, Recent advances in the application of cellulose nanocrystals, Curr. Opin. Colloid Interface Sci. 29 (2017) 32–45.
[24] D. Trache, Nanocellulose as a promising sustainable material for biomedical applications, AIMS Mater. Sci. 5 (2018) 201–205.
[25] H.Y. Yu, D.Z. Zhang, F.F. Lu, J. Yao, New approach for single-step extraction of carboxylated cellulose nanocrystals for their use as adsorbents and flocculants, ACS Sustain. Chem. Eng. 4 (2016) 2632–2643.
[26] S.C. Espinosa, T. Kuhnt, E.J. Foster, C. Weder, Isolation of thermally stable cellulose nanocrystals by phosphoric acid hydrolysis, Biomacromolecules 14 (2013) 1223–1230.
[27] Y. Habibi, L.A. Lucia, O.J. Rojas, Cellulose nanocrystals: chemistry, self-assembly, and applications, Chem. Rev. 110 (2010) 3479–3500.
[28] H. Sadeghifar, I. Filpponen, S.P. Clarke, D.F. Brougham, D.S. Argyropoulos, Production of cellulose nanocrystals using hydrobromic acid and click reactions on their surface, J. Mater. Sci. 46 (2011) 7344–7355.
[29] D. Trache, M.H. Hussin, C.T. Hui Chuin, S. Sabar, M.R.N. Fazita, O.F.A. Taiwo, T. M. Hassan, M.K.M. Haafiz, Microcrystalline cellulose: isolation, characterization and bio-composites application—a review, Int. J. Biol. Macromol. 93 (2016) 789–804.
[30] I.A. Sacui, R.C. Nieuwendaal, D.J. Burnett, S.J. Stranick, M. Jorfi, C. Weder, E.J. Foster, R.T. Olsson, J.W. Gilman, Comparison of the properties of cellulose nanocrystals and cellulose nanofibrils isolated from bacteria, tunicate, and wood processed using acid, enzymatic, mechanical, and oxidative methods, ACS Appl. Mater. Interfaces 6 (2014) 6127–6138.
[31] Y.W. Chen, H.V. Lee, J.C. Juan, S.M. Phang, Production of new cellulose nanomaterial from red algae marine biomass Gelidium elegans, Carbohydr. Polym. 151 (2016) 1210–1219.
[32] A.F. Tarchoun, D. Trache, T.M. Klapötke, M. Derradji, W. Bessa, Ecofriendly isolation and characterization of microcrystalline cellulose from giant reed using various acidic media, Cellulose 26 (2019) 7635–7651.
[33] A.F. Tarchoun, D. Trache, T.M. Klapötke, Microcrystalline cellulose from Posidonia oceanica brown algae: extraction and characterization, Int. J. Biol. Macromol. 138 (2019) 837–845.
[34] H.A. Silvério, W.P. Flauzino Neto, N.O. Dantas, D. Pasquini, Extraction and characterization of cellulose nanocrystals from corncob for application as reinforcing agent in nanocomposites, Ind. Crops Prod. 44 (2013) 427–436.
[35] F. Jiang, Y. Lo Hsieh, Cellulose nanocrystal isolation from tomato peels and assembled nanofibers, Carbohydr. Polym. 122 (2015) 60–68.
[36] J.W. Rhim, J.P. Reddy, X. Luo, Isolation of cellulose nanocrystals from onion skin and their utilization for the preparation of agar-based bio-nanocomposites films, Cellulose 22 (2015) 407–420.
[37] S. Mishra, P.S. Kharkar, A.M. Pethe, Biomass and waste materials as potential sources of nanocrystalline cellulose: comparative review of preparation methods (2016 – Till date), Carbohydr. Polym. 207 (2019) 418–427.
[38] F. Luzi, D. Puglia, F. Sarasini, J. Tirillò, G. Maffei, A. Zuorro, R. Lavecchia, J.M. Kenny, L. Torre, Valorization and extraction of cellulose nanocrystals from North African grass: Ampelodesmos mauritanicus (Diss), Carbohydr. Polym. 209 (2019) 328–337.
[39] M.M.Á.D. Maciel, K.C.C. de C. Benini, H.J.C. Voorwald, M.O.H. Cioffi, Obtainment and characterization of nanocellulose from an unwoven industrial textile cotton waste: effect of acid hydrolysis conditions, Int. J. Biol. Macromol. 126 (2019) 496–506.
[40] S. Naduparambath, T.V. Jinitha, V. Shaniba, M.P. Sreejith, A.K. Balan, E. Purushothaman, Isolation and characterisation of cellulose nanocrystals from sago seed shells, Carbohydr. Polym. 180 (2018) 13–20.
[41] S. Beck-Candanedo, M. Roman, D.G. Gray, Effect of reaction conditions on the properties and behavior of wood cellulose nanocrystal suspensions, Biomacromolecules 6 (2005) 1048–1054.
[42] Y. Zhao, C. Moser, M.E. Lindström, G. Henriksson, J. Li, Cellulose nanofibers from softwood, hardwood, and tunicate: preparation-structure-film performance interrelation, ACS Appl. Mater. Interfaces 9 (2017) 13508–13519.
[43] D. Trache, A. Donnot, K. Khimeche, R. Benelmir, N. Brosse, Physico-chemical properties and thermal stability of microcrystalline cellulose isolated from Alfa fibres, Carbohydr. Polym. 104 (2014) 223–230.
[44] M.A. Mohamed, W.N.W. Salleh, J. Jaafar, S.E.A.M. Asri, A.F. Ismail, Physicochemical properties of "green" nanocrystalline cellulose isolated from recycled newspaper, RSC Adv. 5 (2015) 29842–29849.
[45] M. El Achaby, N. El Miri, H. Hannache, S. Gmouh, H. Ben youcef, A. Aboulkas, Production of cellulose nanocrystals from vine shoots and their use for the development of nanocomposite materials, Int. J. Biol. Macromol. 117 (2018) 592–600.
[46] H.M. Ng, L.T. Sin, T.T. Tee, S.T. Bee, D. Hui, C.Y. Low, A.R. Rahmat, Extraction of cellulose nanocrystals from plant sources for application as reinforcing agent in polymers, Compos. Part B Eng. 75 (2015) 176–200.
[47] F. Meng, G. Wang, X. Du, Z. Wang, S. Xu, Y. Zhang, Extraction and characterization of cellulose nanofibers and nanocrystals from liquefied banana pseudo-stem residue, Compos. Part B Eng. 160 (2019) 341–347.
[48] M. El Achaby, N. El Miri, H. Hannache, S. Gmouh, V. Trabadelo, A. Aboulkas, H. Ben Youcef, Cellulose nanocrystals from Miscanthus fibers: insights into rheological, physico-chemical properties and polymer reinforcing ability, Cellulose 25 (2018) 6603–6619.
[49] E. Hafemann, R. Battisti, C. Marangoni, R.A.F. Machado, Valorization of royal palm tree agroindustrial waste by isolating cellulose nanocrystals, Carbohydr. Polym. 218 (2019) 188–198.